

This article was downloaded by:

On: 25 January 2011

Access details: Access Details: Free Access

Publisher Taylor & Francis

Informa Ltd Registered in England and Wales Registered Number: 1072954 Registered office: Mortimer House, 37-41 Mortimer Street, London W1T 3JH, UK



Separation Science and Technology

Publication details, including instructions for authors and subscription information:

<http://www.informaworld.com/smpp/title~content=t713708471>

UO₂ Sorption in Natural Mexican Erionite and Y Zeolite

M. T. Olguín^a; M. Solache^a; M. Asomoza^b; D. Acosta^c; P. Bosch^{ad}; S. Bulbulian^e

^a INSTITUTO NACIONAL DE INVESTIGACIONES NUCLEARES, MÉXICO, D.F. ^b UNIVERSIDAD AUTÓNOMA METROPOLITANA, IZTAPALAPA, MÉXICO, D.F. ^c UNIVERSIDAD NACIONAL AUTÓNOMA DE MÉXICO, INSTITUTO DE FÍSICA, CIUDAD UNIVERSITARIA, MÉXICO, D.F. ^d UNIVERSIDAD AUTÓNOMA METROPOLITANA, IZTAPALAPA MICHOACÁN Y PURÍSIMA APDO, IZTAPALAPA, MÉXICO, D.F. ^e INSTITUTO NACIONAL DE INVESTIGACIONES NUCLEARES, MÉXICO, D.F.

To cite this Article Olguín, M. T. , Solache, M. , Asomoza, M. , Acosta, D. , Bosch, P. and Bulbulian, S.(1994) 'UO₂ Sorption in Natural Mexican Erionite and Y Zeolite', *Separation Science and Technology*, 29: 16, 2161 – 2178

To link to this Article: DOI: 10.1080/01496399408002196

URL: <http://dx.doi.org/10.1080/01496399408002196>

PLEASE SCROLL DOWN FOR ARTICLE

Full terms and conditions of use: <http://www.informaworld.com/terms-and-conditions-of-access.pdf>

This article may be used for research, teaching and private study purposes. Any substantial or systematic reproduction, re-distribution, re-selling, loan or sub-licensing, systematic supply or distribution in any form to anyone is expressly forbidden.

The publisher does not give any warranty express or implied or make any representation that the contents will be complete or accurate or up to date. The accuracy of any instructions, formulae and drug doses should be independently verified with primary sources. The publisher shall not be liable for any loss, actions, claims, proceedings, demand or costs or damages whatsoever or howsoever caused arising directly or indirectly in connection with or arising out of the use of this material.

UO_2^{2+} Sorption in Natural Mexican Erionite and Y Zeolite

M. T. OLGUÍN AND M. SOLACHE

INSTITUTO NACIONAL DE INVESTIGACIONES NUCLEARES
A.P. 18-1027, COL. ESCANDÓN, DELEGACIÓN MIGUEL HIDALGO
C.P. 11801, MÉXICO, D.F.

M. ASOMOZA

UNIVERSIDAD AUTÓNOMA METROPOLITANA, IZTAPALAPA
MICHOACÁN Y PURÍSIMA APDO. POSTAL 55-532
IZTAPALAPA, C.P. 09340, MÉXICO, D.F.

D. ACOSTA

UNIVERSIDAD NACIONAL AUTÓNOMA DE MÉXICO
INSTITUTO DE FÍSICA
CIUDAD UNIVERSITARIA, MÉXICO, D.F.

P. BOSCH

INSTITUTO NACIONAL DE INVESTIGACIONES NUCLEARES
A.P. 18-1027, COL. ESCANDÓN, DELEGACIÓN MIGUEL HIDALGO
C.P. 11801, MÉXICO, D.F.

UNIVERSIDAD AUTÓNOMA METROPOLITANA, IZTAPALAPA
MICHOACÁN Y PURÍSIMA APDO. POSTAL 55-532
IZTAPALAPA, C.P. 09340, MÉXICO, D.F.

S. BULBULIAN

INSTITUTO NACIONAL DE INVESTIGACIONES NUCLEARES
A.P. 18-1027, COL. ESCANDÓN, DELEGACIÓN MIGUEL HIDALGO
C.P. 11801, MÉXICO, D.F.

ABSTRACT

The use of Y zeolite and erionite to remove UO_2^{2+} ions from aqueous solutions has been investigated. The effect of temperature, the concentration of UO_2^{2+} uptake, the diffusion coefficients, and the ion-exchange isotherms were also studied.

X-ray diffraction, thermal analyses, and transmission electron microscopy were used to characterize the solids. The UO_2^{2+} content was determined by neutron activation analysis. The diffusion coefficients are not clearly affected by temperature or concentration. They definitely depend on the structure of each zeolite. The UO_2^{2+} exchange capacities were 0.2037 and 0.7345 meq $\text{UO}_2^{2+}/\text{g}$ for erionite and Y zeolite, respectively. It was found that UO_2^{2+} is exchanged with the cations of the large cavity in Y zeolite. In the case of erionite, UO_2^{2+} is exchanged with the cations localized in sites where the charge densities are very high.

Key Words. Zeolite; Erionite; Ion exchange; Fission products

INTRODUCTION

Although the sorption of UO_2^{2+} ions by zeolites from aqueous solutions has been focused on catalysis and energy transfer problems (1, 2), it can be reoriented to the recovery of UO_2^{2+} (3). Indeed, in wastewaters the radioactive atoms are not only fission products, but uranium is also present as uranyl ions. These uranyl ions are large (3.84 Å) and, hence, the pore size of the zeolite is expected to play an important role in UO_2^{2+} uptake. The aim of this paper is to present the sorption and diffusion properties of uranyl ions in aqueous solutions using a natural erionite from northern Mexico (Agua Prieta) and a synthetic Y zeolite.

Bennett et al. (4) and Harada et al. (5) showed that the erionite framework can be visualized as consisting of columns formed by cancrinite cages joined together by double 6-ring (DGR) units. Each cancrinite cage is linked to adjacent columns by a single 6-ring (SGR) and, hence, 12-ring-channels 6.3 Å in diameter extending over the entire length of the crystal in the *c* direction are formed. The cancrinite cages in each column are alternately rotated by 60°, thereby placing, in this way, SGR units into a main diameter of 2.5 Å; sorption and diffusion proceeds from the large 12-ring channels to the gmelinite cages via 8-ring openings (3.6 Å in diameter) in the *a* direction.

Y zeolite structure is cubic and consists of sodalite cages connected through hexagonal prisms. Figure 1 compares the erionite and Y zeolite structures (6–8).

The characterization of the sodium and uranyl zeolites was carried out by scanning electron microscopy (SEM), conventional transmission electron microscopy (CTEM), x-ray diffraction (XRD), and thermal analyses (DTA, TGA). The amount of exchanged fission products was determined by neutron activation analysis (NAA).

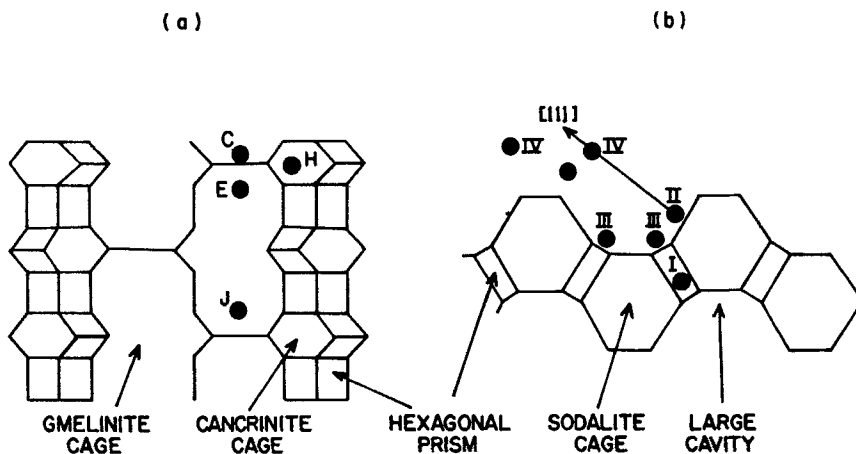


FIG. 1 Cationic sites in (a) erionite: Site C in the center of the six ring, connecting two cancrinite cages, coordinated by three O (5)- and three O (6)-oxygens. Site E analogous to C, but shifted to the gmelinite cage. Site H, in front of the six ring of the cancrinite cage coordinated by two O (2)- and four O (4)-oxygens. Site J, in the gmelinite cage coordinated by two O (4)- and one O (5)-oxygens. (b) Y zeolite: Site I within the hexagonal prism unit. Site II adjacent to the single 6-rings. Site III within the main cavities. Site IV sits in the 12-rings.

EXPERIMENTAL METHODS

1. Materials

Synthetic powdered Y zeolite (Y) (less than 250 mesh) in the Na⁺/NH₄⁺ form was supplied by Valfor [CP301-68; Si/Al = 2.25 (9)]. The erionite (E) was obtained at Agua Prieta, Sonora, and it was powdered to less than 250 mesh. Both zeolites were treated for 8 days in a 5 N NaCl solution washed and dried at 100°C for 5 hours. The sodium content after the treatment was: 1.85 meq Na/g for Y zeolite and 0.8 meq Na/g for erionite.

Analytical grade reagents were used without further purification. UO₂(NO₃)₂ solutions of 0.0010 N (I) and 0.0025 N (II) were used for diffusion experiments, but for ion-exchange isotherms, concentrations were varied from 0.0010 to 0.2000 N.

2. UO₂²⁺ Uptake Curves

Two series of experiments were performed. In the first series, very diluted UO₂(NO₃)₂ solutions were utilized (0.0010 and 0.0025 N) in order to determine the ion-exchange kinetics and the diffusion coefficients. In

the second series, $\text{UO}_2(\text{NO}_3)_2$ solutions from 0.0010 to 0.2000 N were utilized to determine the ion-exchange isotherms. In the second series, crystallinity was partially destroyed when using the more concentrated uranyl nitrate solution.

A. Ion-Exchange Kinetics. Each zeolite sample (150 mg) initially in the Na form was converted partially into the UO_2^{2+} form by the addition of 15 mL of uranyl nitrate solution (either solution I or II). Contact time varied from 3 minutes to 8 days, and two temperatures were chosen (275 and 291 K). The solution was separated from the solid by centrifugation and was then analyzed by the neutron activation technique. The results were plotted as a kinetic curve.

Exchange experiments were labeled with the initials of the zeolite utilized (E or Y), the solution used (I or II), and the temperature used (a or b). For example "curve E1a" corresponds to the uranyl uptake curve in erionite using a 0.0010 N uranyl nitrate solution at 275 K.

B. Diffusion Coefficient Determination. In the crystalline zeolites, ion-exchange kinetics are controlled by diffusion of ions within the aluminosilicate structure. It has been shown that, for spherical particles, the extent of exchange follows (in its initial steps) the relationship (6):

$$\frac{Q_t}{Q_\infty} = \frac{6}{r} \sqrt{\frac{D_i t}{\pi}}$$

where t is the contact time, Q_t and Q_∞ are the exchanged amounts at time t and at equilibrium $t = \infty$, respectively, and r represents the radius of the exchanger particle. In this work r was assumed to be 1.5 μm . This value corresponds to the mean particle size observed in electron microscopy. Q_t/Q_∞ was plotted against time. From the slope of the curve, D_i (apparent diffusion coefficient) was then estimated.

3. Ion-Exchange Isotherms

At 291 K, for a contact time of 24 hours (equilibrium value), both zeolites (200 mg) were exchanged with uranyl nitrate solutions (20 mL, 0.0010 to 0.2000 N). In each case the solution was separated from the solid by centrifugation and was analyzed by neutron activation.

The results were plotted as $(\text{UO}_2^{2+})_z$ against $(\text{UO}_2^{2+})_s$ which are defined as follows:

$$(\text{UO}_2^{2+})_z = \frac{\text{number of equivalents of } \text{UO}_2^{2+} \text{ cation}}{\text{total equivalents of cations in the zeolite}}$$

and

$$(\text{UO}_2^{2+})_s = 2m_s^{\text{UO}_2^{2+}}/2m_s^{\text{UO}_2^{2+}} + m_s^{\text{Na}}$$

where *z* refers to the zeolite and *s* to the solution and *m*_{*s*} values are the molarities in the equilibrium solution, and

$$(UO_2^{2+})_z + (Na^+)_z = 1$$

$$(UO_2^{2+})_s + (Na^+)_s = 1$$

The separation factor $\alpha_{Na^+}^{UO_2^{2+}}$ which expresses the preference of the zeolite for Na⁺ or UO₂²⁺ ions, is defined by

$$\alpha_{Na^+}^{UO_2^{2+}} = (UO_2^{2+})_z(Na^+)_s / (UO_2^{2+})_s(Na^+)_z$$

Note that if the meq UO₂²⁺ exchanged is equal to the meq Na⁺ exchanged, then $\alpha_{Na^+}^{UO_2^{2+}} = 1$, and the exchange obeys the law of mass action (6).

4. Characterization Techniques

A. X-Ray Diffraction. Powder diffractograms were obtained with a Siemens D500 diffractometer coupled to a copper anode tube. Conventional diffractograms were used to identify compounds and to verify crystallinity. Cell parameters in the case of Y zeolite (cubic symmetry) were estimated from the (642) reflection, using a graphite internal standard. To determine the cell parameters of erionite (hexagonal symmetry), graphite was also used as an internal standard and the (210) and (104) peak positions were measured.

B. Neutron Activation Analysis. UO₂²⁺ content in the zeolites was determined by using neutron activation analysis to measure the presence of the remaining uranium in the liquid phase. Aliquots of 1 mL of the original and waste solutions in the TRIGA MARK III reactor were irradiated for 30 seconds with an approximate neutron flux of 10¹³n/cm²s.

The photopeaks of 279 keV from Np²³⁹ produced by the nuclear reaction U²³⁸(n,γ) $\xrightarrow{\beta^-}$ Np²³⁹ were detected with a Ge/hyperpure solid-state detector coupled to a 4096 channel pulse height analyzer.

C. Thermal Analyses. The exchanged Y zeolite (0.630 meq UO₂²⁺/g) and erionite (0.200 meq UO₂²⁺/g) were studied by DTA. A Shimadzu DT-30 thermoanalyzer was operated in an N₂ atmosphere and at a heating rate of 20 K/min from 291 to 1173 K. The reference sample used for DTA analyses was corundum (α-Al₂O₃).

D. Transmission Electron Microscopy. For conventional transmission electron microscopy (CTEM) observations, samples in each case were ground in an agate mortar and then dispersed in isopropyl alcohol for several minutes in an ultrasonic bath. Some drops were deposited on 200 mesh copper grids covered previously with an amorphous carbon film.

Observations were carried out in a side entry JEOL 100CX electron microscope equipped with a goniometer stage. The samples were observed in bright field, dark field, and selected area electron diffraction (SAED) modes at 100 kV in all cases.

For scanning electron microscopy (SEM) observations, the samples were mounted directly on the holders, covered by sputtering with gold, and then observed at 10 and 20 kV in a JEOL 5200 electron microscope.

RESULTS AND DISCUSSION

1. UO_2^{2+} Uptake and Diffusion Coefficients

UO_2^{2+} uptake in the zeolites was monitored for 1 week as shown in Figs. 2 and 3. All these curves attain their equilibrium values after a contact time of approximately 30 minutes. The equilibrium uptake value for curve Ela is 0.050 ± 0.004 meq UO_2^{2+} /g of erionite. This value is 1.36 times smaller than the equilibrium value found for curve Elb (0.068 ± 0.003 meq UO_2^{2+} /g of erionite). The equilibrium UO_2^{2+} uptake value increases considerably when the concentration of the $\text{UO}_2(\text{NO}_3)_2$ solution is increased from 0.068 (Elb) to 0.075 (ElIb). These results show that both temperature and uranyl nitrate solution concentration determine the amount of UO_2^{2+} ion uptake process in erionite; the higher these parameters, the higher the amount of UO_2^{2+} ions sorbed by the zeolites.

The curves obtained with Y zeolite, Fig. 3, very rapidly attain their equilibrium value (less than 2 minutes). The equilibrium UO_2^{2+} uptake value is about 0.092 for both temperatures (0.090 for curve YIa and 0.094 meq/g of Y zeolite for curve YIb). However, the equilibrium UO_2^{2+} uptake value increases considerably from curve YIb to curve YIIb (0.094 and 0.218 meq/g) if the UO_2^{2+} nitrate solution concentration is increased from 0.0010 to 0.0025 N. The UO_2^{2+} uptake value is only dependent on the uranyl solution concentration for the temperature and concentration values studied.

The diffusion coefficient values (D_i) can be grouped in two intervals. The first one is for curves Ela, Elb, and ElIb, defined by the values $1.0 \pm 0.3 \times 10^{-11}$ cm²/s, and the second for curves YIa, YIb, and YIIb, with D_i values higher than 1.0×10^{-11} cm²/s. Andreeva et al. (11) obtained (from UO_2^{2+} solutions with pH 2–4) a D_i value of 1.1×10^{-13} cm²/s for mordenite and clinoptilolite. It therefore seems that diffusion of UO_2^{2+} in erionite is 100 times faster than in mordenite and clinoptilolite. Such a difference might be attributed to different particle sizes and structures.

Depending on the initial UO_2^{2+} concentration and the pH, different uranyl–hydroxo complexes must be considered in aqueous solutions. The predominant species at the various pH values are the following: pH 4,

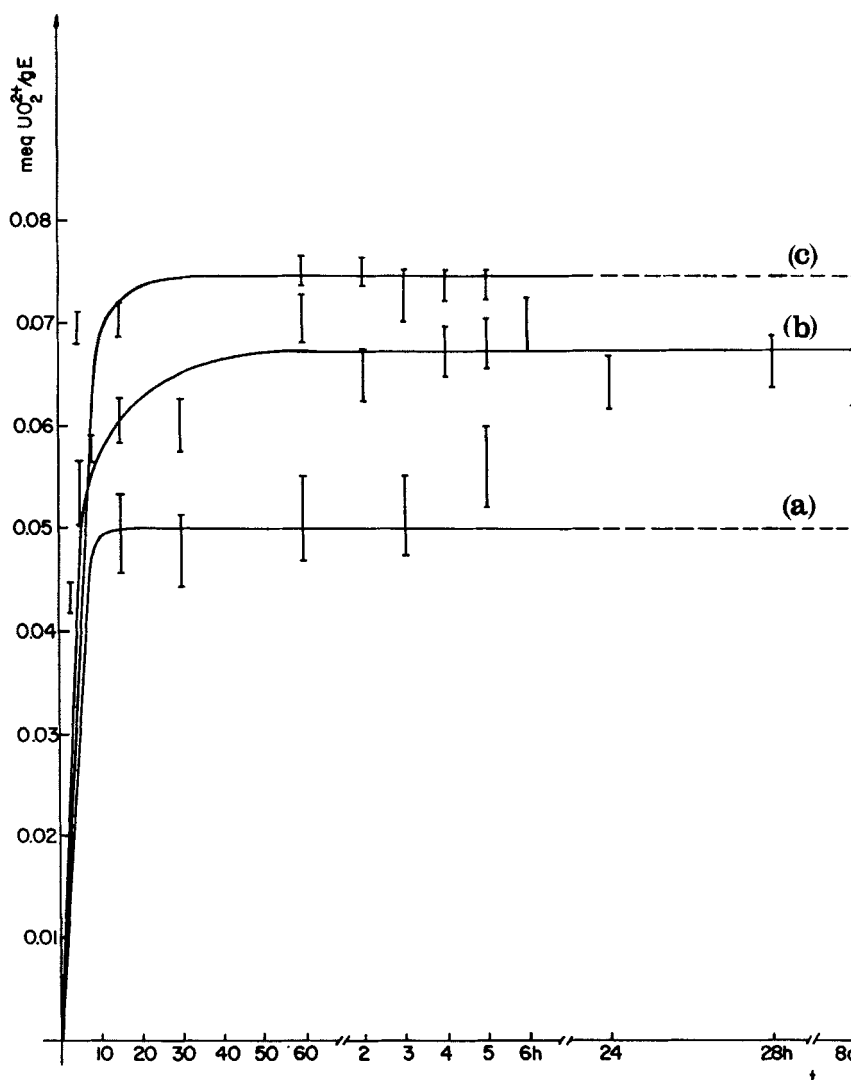


FIG. 2 UO₂²⁺ uptake curve in erionite. (a) At 275 K with 0.0010 N uranyl nitrate solution, EIa; (b) at 291 K with 0.0010 N uranyl nitrate solution, EIb; (c) at 291 K with 0.0025 N uranyl nitrate solution, EIb.

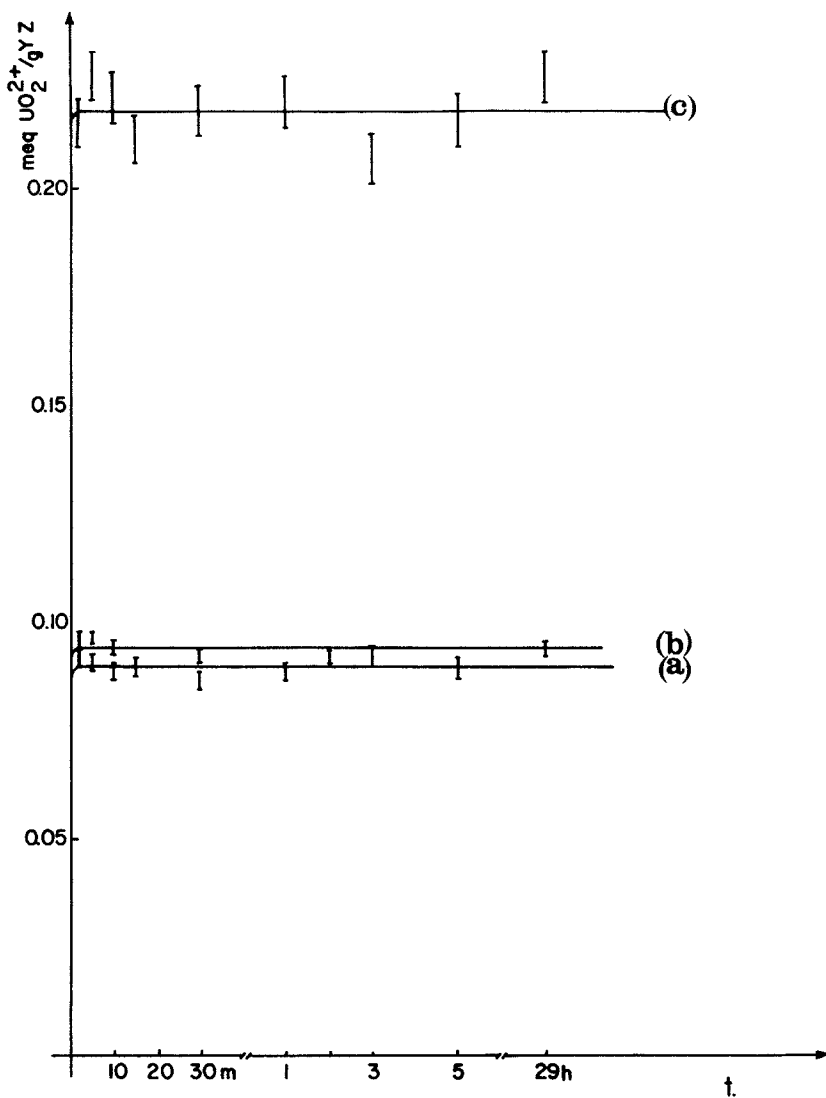


FIG. 3 UO_2^{2+} uptake curve in Y zeolite. (a) At 275 K with 0.0010 N uranyl nitrate solution, YIa; (b) at 291 K with 0.0010 N uranyl nitrate solution, YIb; (c) at 291 K with 0.0025 N uranyl nitrate solution, YIIb.

UO₂²⁺; pH 5.5, UO₂(OH)⁺ and (UO₂)₂(OH)₂²⁺; pH 6, (UO₂)₃(OH)₈⁺. Vochten et al. (12) showed that in our working conditions (pH 4) the predominant species present during the diffusion process is UO₂²⁺.

2. Ion-Exchange Isotherms

Figures 4 and 5 show the ion-exchange isotherms obtained with erionite and Y zeolite, respectively. In both cases complete exchange is not attained as the isotherms lie below the diagonal line and the corresponding separation factor becomes $\alpha < 1$. For Y zeolite, the expected isotherm was obtained. However, in erionite the selectivity varies with the degree of exchange and a sigmoidal isotherm results.

The maximum (UO₂²⁺)_z values obtained for erionite and Y zeolite were about 0.3 and 0.4, respectively, which means that the ion-exchange capacity of both zeolites is quite low. These obtained values for (UO₂²⁺)_z indicate one of the following possibilities: a) because of their size, the UO₂²⁺ ions cannot enter some of the cages and interconnecting channels within the zeolite structure, b) the ion sieving phenomenon can also be accompanied by a volume exclusion effect (13). In this case, no more room is left in the cavities to accommodate all UO₂²⁺ ions. Finally, c), hydrolysis can produce hydronium ions that compete with UO₂²⁺ ions for cationic sites.

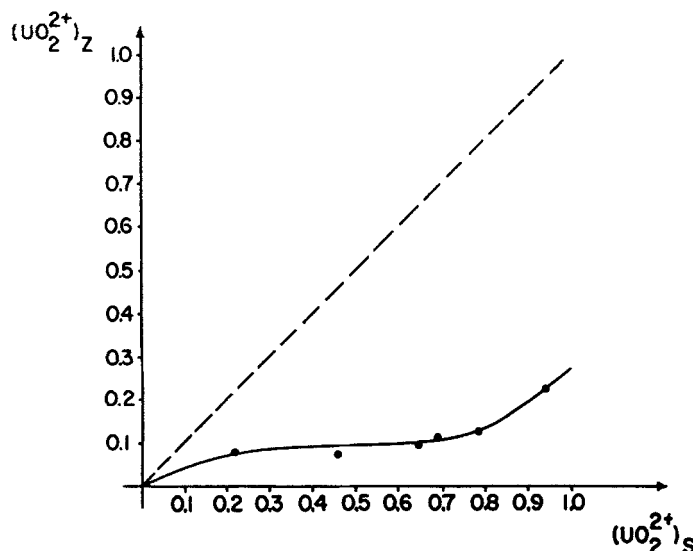


FIG. 4 Ion-exchange isotherms in erionite, UO₂²⁺ concentration in zeolite [(UO₂²⁺)_z] vs UO₂²⁺ concentration in the equilibrium solution [(UO₂²⁺)_s].

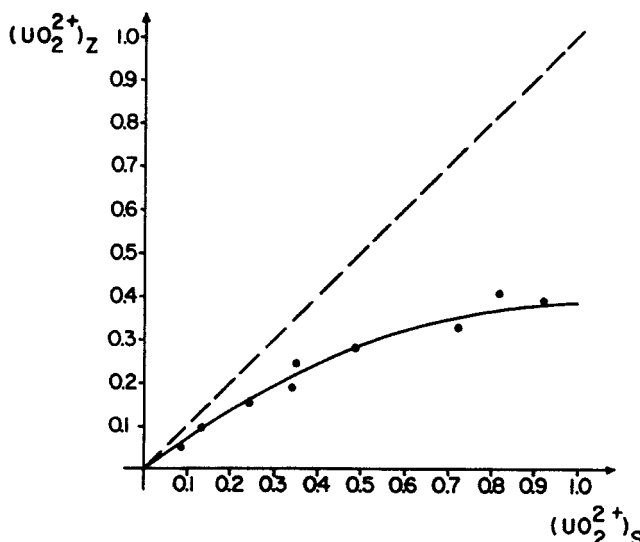


FIG. 5 Ion-exchange isotherms in Y zeolite, $(\text{UO}_2^{2+})_z$ concentration in zeolite vs $(\text{UO}_2^{2+})_s$ concentration in the equilibrium solution.

In Y zeolite, cations in site 1 in the hexagonal prisms are the most difficult to exchange. Most probably, UO_2^{2+} ions are excluded from these sites owing to their considerable size (3.84 Å). In fact, they are too large under normal conditions to pass through the 2.4 Å diameter opening. The isotherm for the exchange levels off at $(\text{UO}_2^{2+})_z = 0.4$, which can be understood as follows: 35 of the 59 univalent ions in the unit cell are not exchanged, 16 of these ions correspond to the 16 site I ions located within the double 6-ring, and the remainder correspond to ions in site II, i.e., the exchangeable UO_2^{2+} ions are located in the most accessible cation sites, III and IV in the large cavity, Fig. 1.

For erionite, the $(\text{UO}_2^{2+})_z$ value is 0.3. This means that only 30% of the total exchangeable sites per unit cell are occupied by the uranyl ions in this zeolite. These sites, according to Roessner et al. (7), are most probably the C, E, and H sites where charge densities are indeed very high. According to these authors, divalent cations have been found to be located preferentially in those positions, and they again represent 30% of the total exchangeable sites.

3. Characterization

A. X-Ray Diffraction. In the samples used to determine ion-exchange isotherms it was observed that crystallinity was maintained only when

using dilute uranyl nitrate solutions (up to 0.0100 N for Y zeolite and 0.0030 N for erionite). The samples exchanged with the highest uranyl nitrate concentrations partially lost their crystallinity. The lattice parameters for the Na⁺ and UO₂²⁺ exchanged erionite samples (Table 1) were altered only at high concentration of UO₂²⁺ ion (0.2 meq/g). In this sample, parameter a_0 remained constant but parameter c_0 shrank from 15.01 to 14.96 Å. Lattice parameters were expected to expand because the ionic radii of sodium and uranyl are 0.9 and 3.84 Å, respectively. However, the experimental evidence showed that the lattice shrinks with exchange. Two hypothesis can be proposed. First, uranyl ions may be interacting with two opposite windows since it is very large. For instance, it may be located in site J in the gmelenite cage not only coordinated by the two O(4) and one O(5) oxygens but also by the three O(5) and the three O(6) oxygens characteristic of the E site (7). Second, sodium may be expelled but not necessarily exchanged by UO₂²⁺; hydronium ion-lattice interactions could also be expected in the structure. Since the measured lattice parameters are an average between the expansion (or contraction) due to UO₂²⁺ present and to the contraction due to H⁺ exchange, and if the UO₂²⁺ exchange amount is lower than that from hydronium ion exchange, the average lattice parameter would shrink. This hypothesis may be verified with neutron activation analysis.

UO₂²⁺ concentrations (up to 0.63 meq/g) in Y zeolite do not alter the lattice parameters (Table 2), showing that either the UO₂²⁺ is not exchanged by the cations of Y zeolite, and therefore do not occupy cationic sites in the zeolites, or that UO₂²⁺ ions occupy the large cavity where, due to its very large diameter, the parameters are not affected by the presence of UO₂²⁺ ions.

B. Neutron Activation Analysis. Table 3 shows the UO₂²⁺ sorption in erionite and Y zeolite and Na⁺ found in uranyl nitrate solution after the ion-exchange process. Results show that for each Na⁺ equivalent removed from the erionite, only a fraction of UO₂²⁺ equivalents is introduced into it. This fraction of about 0.5 for dilute solutions increases with the

TABLE 1
Cell Parameters of Erionite Before and After
UO₂²⁺ Ion Exchange (0.200 meq UO₂²⁺/g)

Sample	Cell parameters (Å)	
	a_0	c_0
E(Na ⁺)	13.159	15.012
E(UO ₂ ²⁺)	13.163	14.963

TABLE 2
Cell Parameters of Y Zeolite Before and After
 UO_2^{2+} Ion Exchange (0.630 meq UO_2^{2+} /g)

Sample	Cell parameter (Å), a_0
$\text{Y}(\text{Na}^+)$	24.690
$\text{Y}(\text{UO}_2^{2+})$	24.680

TABLE 3
a) UO_2^{2+} Sorption in Erionite and Y Zeolite Exchanged with Uranyl Nitrate Solution;
(b) Na^+ Found in Uranyl Nitrate Solution after the Ion-Exchange Process

	Concentration (N)	Uranyl nitrate samples	
		(a) meq UO_2^{2+} /g	(b) meq Na^+ /100 mL
Y	0.0010	0.0914	0.0931
	0.0020	0.1749	0.1718
	0.0030	0.2111	0.2059
	0.0040	0.2948	0.2984
	0.0050	0.3220	0.3367
	0.0075	0.4617	0.5085
	0.0100	0.5060	0.5260
	0.0300	0.6275	0.9000
	0.0500	0.7925	0.9430
	0.1000	0.7345	0.8745
E	0.0010	0.0670	0.1300
	0.0020	0.0631	0.1650
	0.0060	0.1000	0.2715
	0.0100	0.1048	0.4250
	0.0200	0.0975	0.6239
	0.2000	0.2037	1.4780

concentration of the uranyl nitrate solution. The same effect has been found by Franklin et al. (14) when studying Mg^{2+} exchange in NaY zeolite. They reported that a considerable percentage of Na^+ ions is exchanged by hydronia produced during hydrolysis. The levels of hydronia were inferred from the difference between the total analyzed exchangeable cation content and the exchange capacity based on the aluminum content of the sample. We therefore conclude that during UO_2^{2+} ion exchange, a considerable percentage of Na^+ ions was exchanged by hydronia ions produced during hydrolysis. These results confirm the second hypothesis proposed in the X-Ray Diffraction Section. This conclusion does not mean

that UO₂²⁺ is not incorporated into the network. X-ray diffraction results correspond to an average over all the sample.

Concerning the x-ray diffraction results for UO₂²⁺-exchanged Y zeolite, the uncertainty about the position of UO₂²⁺ in the zeolite can be solved by studying the Na⁺ ions displaced from Y zeolite and the UO₂²⁺ ions introduced into the zeolite. The results show that for every UO₂²⁺ ion sorbed by the Y zeolite, an equivalent amount of Na⁺ ions has been displaced from it. This result shows that UO₂²⁺ is certainly exchanged in Y zeolite. We have to conclude that in this case UO₂²⁺ ions are located in the large cavity and therefore the cell parameter is not altered. This is consistent with other reports (1, 2, 12).

C. Thermal Analysis. DTA results for Na⁺- and UO₂²⁺-exchanged erionite and Y zeolite are as follows. A peak was found at 393 K. It corresponds to nonexchanged erionite and it is interpreted as due to the expected water loss. If this zeolite exchanges Na⁺ for UO₂²⁺, this peak shifts to 363 K and becomes sharper. It seems, then, that UO₂²⁺ weakens the H₂O bonds in the zeolite structure. Hence, in this case water is eliminated at a lower temperature. This effect is not found if Y zeolite exchanges Na⁺ for UO₂²⁺. The DTA curves confirm that the nature of the exchanged cation may exert an important influence on the stability and dehydration behavior of the zeolite. Furthermore, the exchanged zeolites are stable from 300 to 1173 K. It has been shown that for chabazite, as the size of the univalent cation increases, the temperature at which the water is lost increases (6).

D. Electron Microscopy. The morphology and structure of the natural and exchanged erionite were studied by electron microscopy.

From CTEM images, the samples present two basic configurations in all cases:

1. Laminar configurations (or planar crystals) with regular geometry, marked A in Fig. 6.
2. Agglomerates of erionites with irregular configuration, marked B in Fig. 6.

In bright and dark field images, no significant modifications in the morphology were detected from one sample to the other.

From SAED patterns, an analysis on the evolution of samples with impregnation time was achieved. In all cases the presence of erionite with a high degree of crystallinity was detected (Fig. 7). The coincidence of the measured interplanar distances with those reported in the JCPDS cards 12-275 and 39-1379 are better than 90% (95% in some cases). If interplanar distances are compared with JCPDS card 20-832, the presence of offretite in a low concentration (less than 1%) is shown.

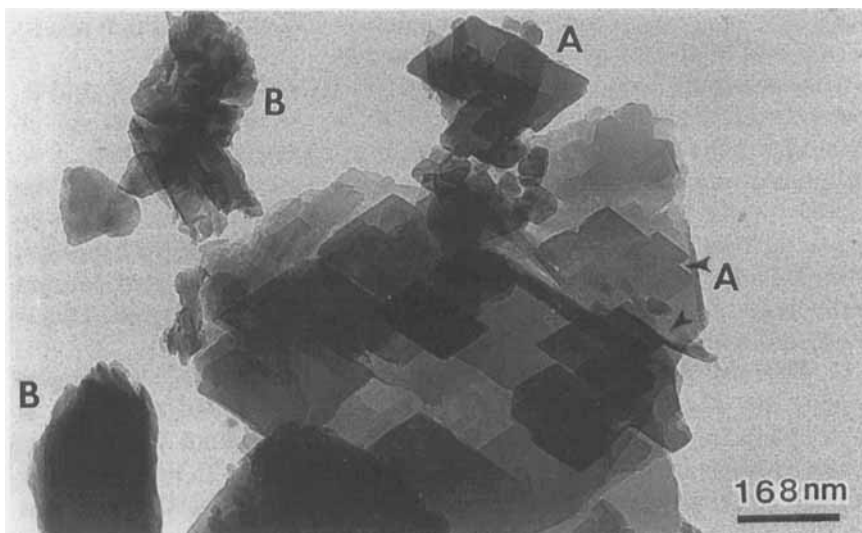


FIG. 6 CTEM images of erionite exchanged with UO_2^{2+} ions (0.067 meq $\text{UO}_2^{2+}/\text{g}$).

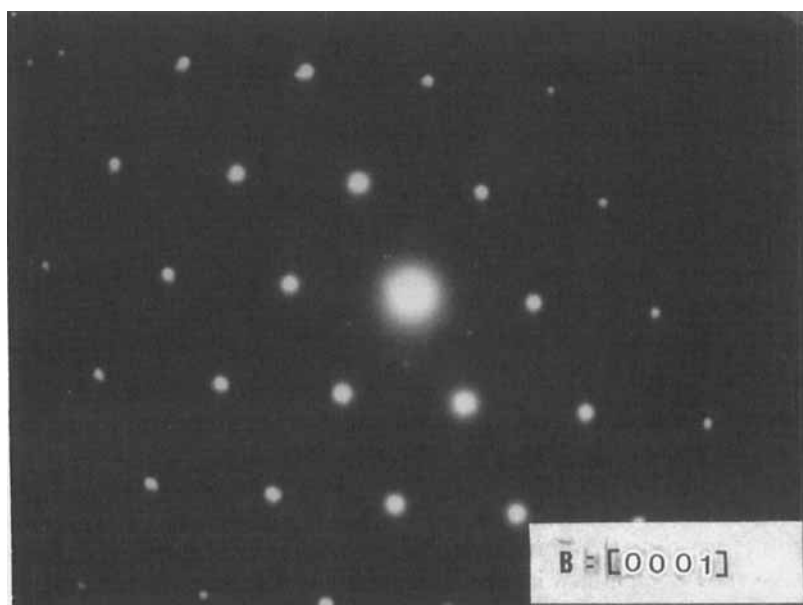


FIG. 7 Diffraction pattern of erionite exchanged with UO_2^{2+} ions (0.0010 N solution and a contact time of 24 hours).

Table 4 shows a comparison between interplanar distances for the sample left in contact for 8 days with those of JCPDS 12-275 and 39-1379 cards.

These results might indicate that diffusion of uranyl ions inside the erionite lattice induces local changes in the initial structure.

TABLE 4

Interplanar Distances for Erionite Exchanged with UO₂²⁺ Ions Left in Contact for 8 Days in 0.001 N Solution in Comparison to JCPDS 12-275 and 39-1379 Cards

Exchanged erionite (8 days), <i>d</i> (Å) ± 0.02	JCPDS cards	
	12-275, <i>d</i> (Å)	39-1379, <i>d</i> (Å)
9.89	—	—
9.71	—	—
7.25	—	—
6.04	—	—
4.53	4.56	4.54
4.31	4.32	4.36
4.25	4.32	4.18
3.16	3.17	3.15
3.09	3.10	2.93
2.30	2.28	2.41

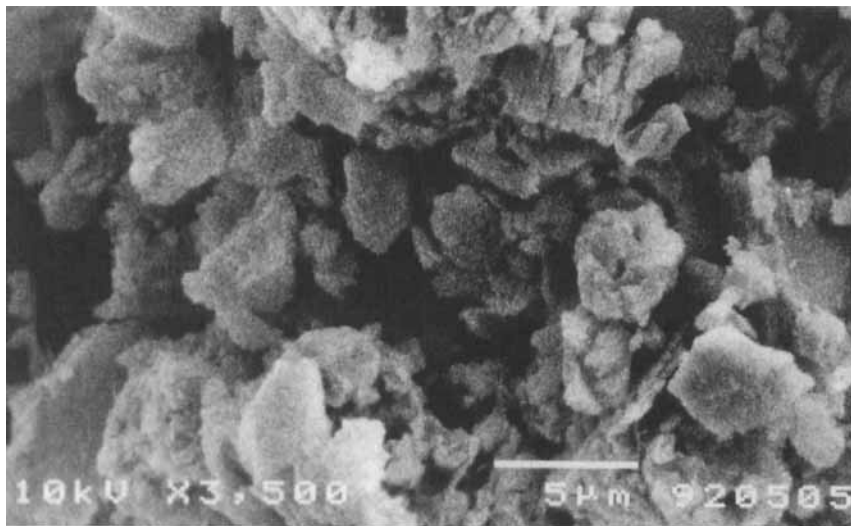


FIG. 8A SEM images of erionite. Natural erionite crystallites.

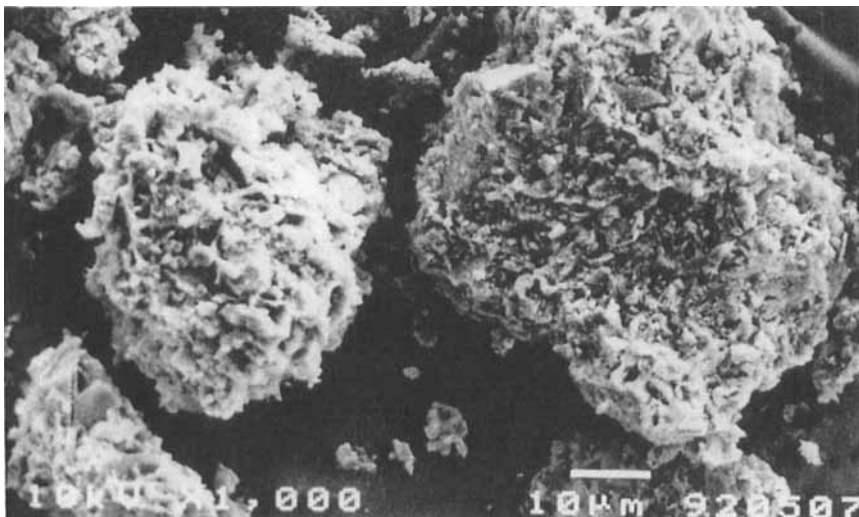


FIG. 8B Uranyl exchanged erionite, 0.0010 N uranyl solution and a contact time of 5 minutes.

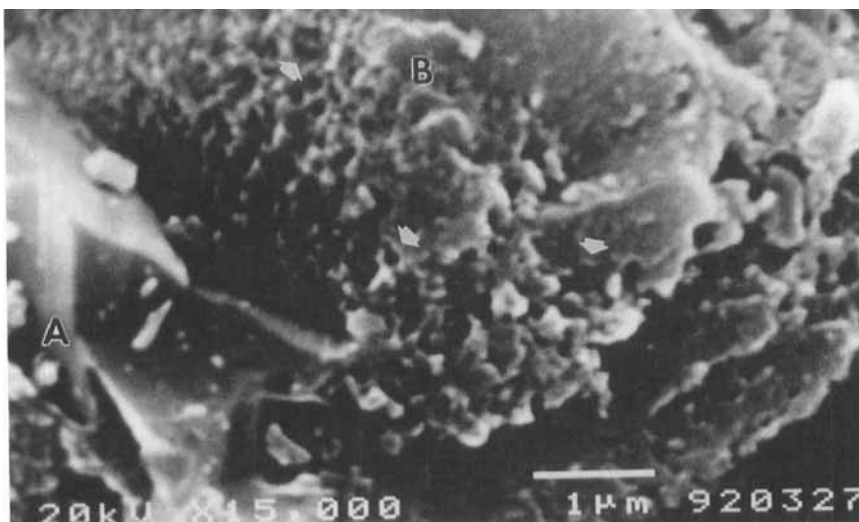


FIG. 8C Uranyl exchanged erionite, 0.0010 N uranyl solution and a contact time of 8 days.

SEM images reveal that surface modifications in the crystals of the zeolite are generated as a consequence of contact time with 0.0010 N uranyl solution, as can be appreciated in Figs. 8A, 8B, and 8C. Figure 8A shows an image of agglomerates of natural erionite. Figure 8B shows an image of a uranyl sample (contact time of 5 minutes). In this figure, erionite crystals with a high number of aggregates on their surfaces are observed. Figure 8C shows an image from a uranyl sample (contact time of 8 days). This figure shows two kinds of crystals. One of them, crystal A, does not show any noticeable surface modifications, and crystal B shows pores and other surface modifications.

CONCLUSIONS

UO₂²⁺ uptake results show that in a temperature range of 275–291 K and concentration values of 0.0010 and 0.0025 N, the exchange temperature is an important parameter for UO₂²⁺ exchange in erionite, and the concentration of uranyl nitrate solution is a critical one. The more concentrated the uranyl nitrate solution, the higher the UO₂²⁺ uptake. In Y zeolite, temperature does not play an important role; the most important parameter is the concentration of uranyl nitrate. The diffusion coefficient definitely depends on the structure of each zeolite, with those found for Y zeolite being much higher than those found for erionite.

Uranyl ions have been truly exchanged in erionite, most probably in the C, E, and H sites where charge densities are very high. However, not all Na⁺ ions leaving from the erionite sample have been exchanged with UO₂²⁺; most have been exchanged with hydronium ions produced during hydrolysis.

It was also shown that uranyl ions can be exchanged with Na⁺ ions occupying the large cavity in Y zeolite (sites III or IV). We have found that these uranyl-exchanged Y zeolite and erionite materials are thermally stable to temperatures of 1173 K.

ACKNOWLEDGMENTS

We acknowledge financial support from CONACyT and the Cyted-D program, and we thank V. H. Lara (UAM), J. Cañetas (IFUNAM), and the technicians of the Chemistry Department (ININ) for technical help.

REFERENCES

1. S. L. Suib and K. A. Carrado, *Inorg. Chem.*, **24**, 200 (1985).
2. S. L. Suib and K. A. Carrado, *Ibid.*, **24**, 863 (1985).

3. Y. Legoux, G. Blain, R. Guillaumont, G. Ouzounian, L. Brillard, and M. Hussonnois, *Radiochim Acta*, Special Issue 58/59, Part II, p. 211 (1992).
4. J. M. Bennett and J. A. Gard, *Nature*, **214**, 1005 (1967).
5. H. Harada, I. Shigeki, and K. Kuniaki, *Am. Mineral.*, **52**, 1785 (1967).
6. W. Breck, *Zeolite Molecular Sieves*, Wiley-Interscience, New York, 1974.
7. F. Roessner, K. H. Steinberg, A. Rudolf, and B. Staudte, *Zeolites*, **9**, 371 (1989).
8. K. P. Lillerud and J. H. Raeder, *Ibid.*, **6**, 474 (1986).
9. I. García-S. and M. Solache-Ríos, Personal Communication.
10. G. Aguilar, J. Aguilar, G. Díaz, A. De Ita, and A. Maubert, Informe semestral (CyTED-D), 1991.
11. N. R. Andreeva and N. B. Chernyavskaya, *Radiokhimiya*, **24**, 9 (1982).
12. R. F. C. Vochten, L. Haverbeke, and F. J. Goovaerts, *J. Chem. Soc., Faraday Trans. I*, **86**, 4095 (1990).
13. R. P. Townsend, "Ion Exchange in Zeolites," Chapter 10 in *Introduction to Zeolite Science and Practice* (H. Van Bekkum, E. M. Flanigen, and J. C. Jansen, Eds.), Elsevier, Amsterdam, 1991.
14. K. R. Franklin and R. P. Townsend, *J. Chem. Soc., Faraday Trans. I*, **84**, 2755 (1988).

Received by editor March 25, 1993

Revised January 24, 1994

Rerevised March 14, 1994